13.2

Study of the electrochemical properties of a supercapacitor electrode based on nickel oxide of vacuum-arc synthesis

© I.V. Karpov[1,2], A.V. Ushackov[1,2], L.Yu. Fedorov[1,2], E.A. Goncharova[2], A.A. Shaihadinov[2]

[1] Krasnoyarsk Scientific Center of the Siberian Branch of the Russian Academy of Sciences, Krasnoyarsk, Russi
[2] Siberian State University, Krasnoyarsk, Russia
E-mail: sfu-unesco@mail.ru

Received November 14, 2022
Revised August 9, 2023
Accepted November 6, 2023

The working electrode of the electrochemical cell was obtained by vacuum-arc deposition of NiO nanoparticles on a graphite plate in an argon/oxygen atmosphere. The measurements were carried out using a two-electrode scheme. The electrochemical properties of the fabricated electrode (as part of an electrochemical cell) were studied using the electrochemical impedance method, cyclic voltammetry and galvanostatic charge-discharge. 6 M KOH was used as the electrolyte.

Keywords: nickel oxide, vacuum arc, pseudocapacitance, supercapacitor.

DOI: 10.61011/PJTF.2024.03.57036.19428

The ease of obtaining nanoscale transition metal oxides along with their unique physical properties has predetermined a wide research interest in them. Such materials find technological applications in high-sensitivity sensors [1], hard electrolytes [2], and supercapacitors [3].

Electrochemical activity of nickel oxide in interaction with electrolytes creates conditions for reversible oxidation-reduction reactions [4,5]. This enables pseudocapacitive charge storage in addition to the capacitance of the electrical double layer. In this way, high energy storage rates are achieved. In general, for active pseudocapacitor materials, chemical and thermal stability is essential. Nickel oxide has these features, and its capacitive characteristics are now widely investigated for a large variety of morphologies, and when obtained by various methods [6,7]. This provides a reduction in ion diffusion length, as well as an increase in electrolyte penetration.

The background for the present work was the studies of the effect of quenching rate on the crystalline and impedance properties of NiO nanoparticles [8]. It was found that an increase in the quenching rate leads to a significant strengthening of the role of morphology and crystalline structure of the surface layer of nanoparticles: the powder becomes X-ray amorphous, dielectric permittivity increases to giant values, and conductivity is transformed from electronic to ionic one.

To fabricate the electrodes, NiO nanopowder was deposited on graphite plates by plasma-chemical synthesis in a low-pressure arc reactor [9]. A high-purity nickel (99.99%) cathode with a diameter of 80 mm and a length of 100 mm was used, which was mounted on a water-cooled nickel current lead. The arc vaporizer had the following characteristics: arc discharge current of 100 A, longitudinal magnetic field strength on the cathode surface created by the focusing coil, 80 A/m, the distance between the cathode and anode was 50 mm. To carry out plasma-chemical reactions, a gas mixture (20 vol.% O_2 from the supply of plasma-forming gas Ar) was injected into the chamber after pre-pumping to the pressure $3 \cdot 10^{-4}$ Pa. The deposition of nanoparticles was carried out at a base pressure of 180 Pa. Oxygen was fed into the reactor in such a way as to form a homogeneous envelope around the plasma torch.

To investigate the morphology, phase composition, etc., a witness sample of NiO nanopowder was obtained separately. The shape of the obtained nanoparticles is close to spherical. The powder had almost stoichiometric composition ($Ni_{48}O_{52}$), the crystal structure corresponds to face-centered cubic lattice (fcc), and the average size of the coherent scattering regions is 18 nm. More detailed structural and morphological studies of NiO nanoparticles are presented in Ref. [8]. The amount of precipitated nickel oxide was determined by the mass change of the graphite electrode on an analytical balance; it was 0.035 g/cm^2.

The electrochemical behavior of the samples was studied using a potentiostat-galvanostat P-45X with a frequency analyzer module „FRA-24M“ (Electrochemical Instruments, Russia). Impedance measurements were performed in the frequency range from 10 mHz to 100 kHz using a two-electrode scheme. Graphite plates (ACS 7-3, purity of 99.999%) were used as electrode materials. Filter paper impregnated with aqueous electrolyte 6 M KOH (C.P.) was used as a separator.

The area of the graphite electrodes was 1.27 cm^2. The studies were carried out using a two-electrode twisting cell. The device consists of the cell itself, two nuts, two current collectors, electrodes and sealing gaskets. The cell assembly was carried out in a glove box in an argon environment.

The experimental impedance spectra are shown in Fig. 1. The points of the locus form a well-defined half-circle arc (lower inset) at high frequencies and an increasing low-

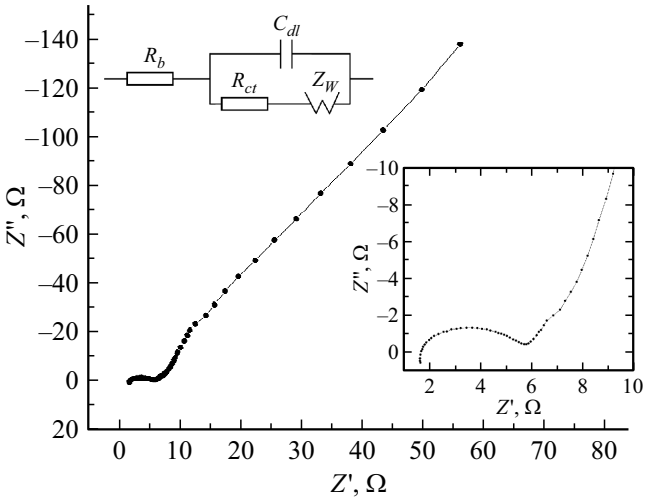

Figure 1. Impedance locus of an electrochemical cell. The upper inset shows — equivalent scheme (high frequency region of the locus).

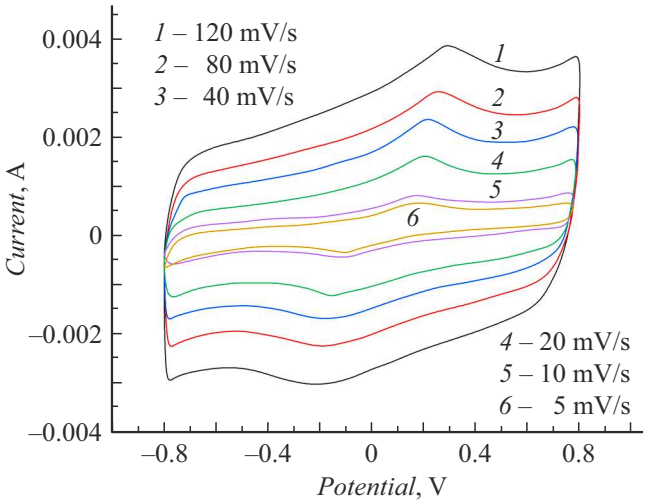

Figure 2. Cyclic voltammogram of an electrochemical cell at different potential sweep rates.

frequency beam, which first tends almost vertically upward, and then (in the lower frequency range) changes slope, which confirms the formation of a double layer at the electrode–electrolyte boundary, and also proves the capacitive nature of the double layer in the interfacial region. For numerical approximation of this locus, the equivalent electrical scheme shown in the upper inset to Fig. 1 is well suited. It includes contact resistance $R_b = 0.45\,\Omega \cdot \mathrm{cm}^2$, double layer capacitance $C_{dl} = 3.17\,\mu\mathrm{F} \cdot \mathrm{cm}^{-2}$, charge transfer resistance $R_{ct} = 0.78\,\Omega \cdot \mathrm{cm}^2$, and Warburg component $Z_W = 0.9\,\Omega \cdot \mathrm{cm}^2$.

As can be seen, the low value of the bulk resistance (R_b) of the electrode material and current collector material is due to the conductive nature and the interface with low transient resistance between them. In addition, the low value of charge transfer resistance (R_{ct}) indicates rapid charge transfer at the electrode–electrolyte interfaces and ionic conductivity of the liquid electrolyte, which implies better accessibility of the pores of the NiO working electrodes to the electrolyte ions and hence higher capacitance value. In addition, the porous structure of the NiO working electrodes allows electrolyte penetration into the inner volume of the electrode, thereby improving the electrode–electrolyte contact and hence reducing the internal resistance.

Cyclic voltammetry (CVA) of the NiO-based electrode is shown in Fig. 2. Measurements were carried out at different potential sweep rates varying from 5 to 120 mV/s. As can be seen from the CVA-curves, characteristic peaks in the anodic and cathodic regions, most likely related to oxidation $Ni^{2+} \rightarrow Ni^{3+}$ and reduction $Ni^{3+} \rightarrow Ni^{2+}$, are observed at different potential sweep rates in the range from −0.15 to −0.25 V and from +0.15 to +0.25 V. The charge-discharge mechanism explaining the pseudocapacitive behavior of nickel oxide in alkaline media is well known (see e.g. [3,10]). The shape of the CVA-curves is

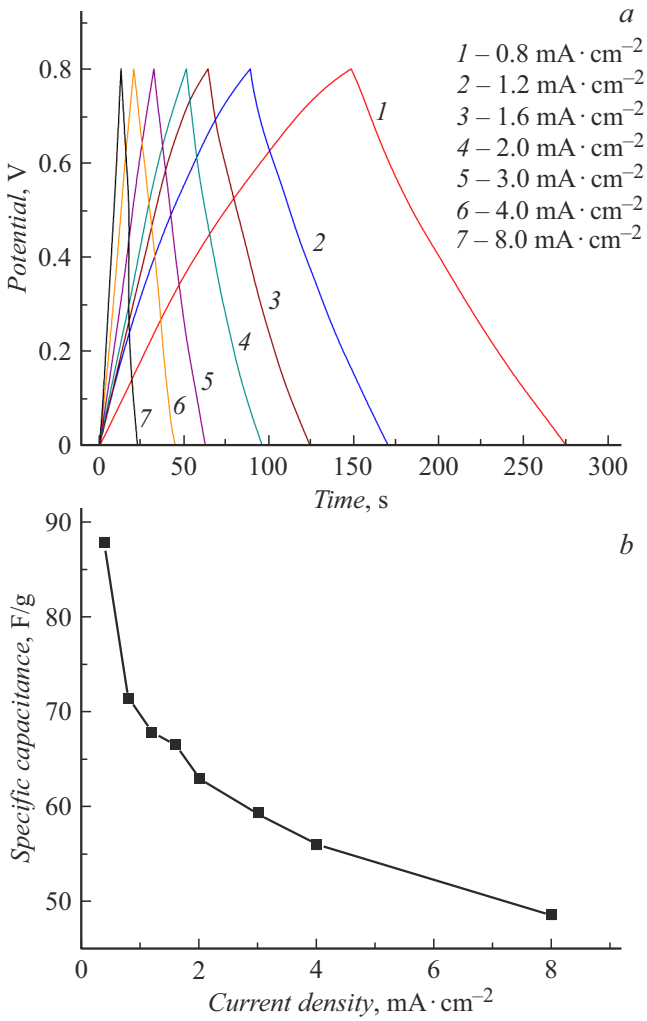

Figure 3. Charge-discharge curves (*a*) and specific capacitance (*b*) of an electrochemical cell at different current densities.

close to rectangular, indicating the main contribution to the capacitance formation due to the electrical double layer.

Based on the measurement results, the capacitance was evaluated for maximum and minimum potential sweep rates. Thus, for a potential sweep rate of 5 mV/s, the capacitance was 560.2 mF/cm^2, which corresponds to a specific electrode capacitance of 280.1 F/g, and at a potential sweep rate of 120 mV/s, the capacitance was 215.7 mF/cm^2, which corresponds to a specific electrode capacitance of 107.8 F/g. A likely reason for the significant decrease in specific capacitance with increasing potential sweep rate may be that the electrochemical process does not keep pace with the change in electrode potential. Therefore, the currents are less and less dependent and then no longer dependent on the sweep rate.

This electrode was also characterized by charge-discharge curves obtained at different current densities (Fig. 3, *a*), from which the specific capacitance of the sample was determined (Fig. 3, *b*). The charge-discharge curves have a triangular shape with a linear discharge profile, which indicates the capacitive nature of the electrical double layer.

Thus, in our study, NiO nanoparticles were successfully obtained by vacuum-arc synthesis. A working electrode was fabricated for electrochemical studies. Impedance spectroscopy showed the capacitive nature of the double layer in the interfacial region. A specific capacitance of about 521.4 mF/cm^2 was obtained, which is equivalent to the specific capacitance of a single electrode (260.7 F/g). The obtained results confirm the possibility of using vacuum-arc synthesis nickel oxide in the creation of electrode materials for pseudocapacitors and create a scientific basis for further research.

Funding

The work has been performed under the state assignment ES-2021-0026.

Conflict of interest

The authors declare that they have no conflict of interest.

References

[1] J. Bartolomé, M. Taeño, R. Martínez-Casado, D. Maestre, A. Cremades, Appl. Surf. Sci., **579**, 152134 (2022). DOI: 10.1016/j.apsusc.2021.152134
[2] M.S. Lee, S. Lee, W. Jeong, S. Ryu, W. Yua, Y.H. Lee, G.Y. Cho, S.W. Cha, Int. J. Hydrogen Energy, **46**, 36445 (2021). DOI: 10.1016/j.ijhydene.2021.08.138
[3] S.D. Dhas, P.S. Maldar, M.D. Patil, A.B. Nagare, M.R. Waikar, R.G. Sonkawade, A.V. Moholkar, Vacuum, **181**, 109646 (2020). DOI: 10.1016/j.vacuum.2020.109646
[4] R.S. Kate, S.A. Khalate, R.J. Deokate, J. Alloys Compd., **734**, 89 (2018). DOI: 10.1016/j.jallcom.2017.10.262
[5] G. Cai, X. Wang, M. Cui, P. Darmawan, J. Wang, A.L.-S. Eh, P.S. Lee, Nano Energy, **12**, 258 (2015). DOI: 10.1016/j.nanoen.2014.12.031
[6] M. Jayachandran, S. Kishore babu, T. Maiyalagan, M.R. Kannan, R. Goutham kumar, Y. Sheeba Sherlin, T. Vijayakumar, Mater. Lett., **302**, 130415 (2021). DOI: 10.1016/j.matlet.2021.130415
[7] S. Verma, S. Arya, V. Gupta, S. Mahajan, H. Furukawa, A. Khosla, J. Mater. Res. Technol., **11**, 564 (2021). DOI: 10.1016/j.jmrt.2021.01.027
[8] A.V. Ushakov, I.V. Karpov, G.M. Zeer, L.Yu. Fedorov, V.G. Demin, E.A. Goncharova, IEEE Trans. Dielectrics Electrical Insulation, **27**, 1486 (2020). DOI: 10.1109/TDEI.2020.009110
[9] A.V. Ushakov, I.V. Karpov, L.Yu. Fedorov, V.G. Demin, E.A. Goncharova, A.A. Shaihadinov, G.M. Zeer, S.M. Zharkov, Physica E, **124**, 114352 (2020). DOI: 10.1016/j.physe.2020.114352
[10] A. Sankar, S.V. Chitra, M. Jayashree, M. Parthibavarman, T. Amirthavarshini, Diamond Relat. Mater., **122**, 108804 (2022). DOI: 10.1016/j.diamond.2021.108804

Translated by D.Kondaurov